

Deciphering the mutational signature of congenital limb malformations

Liyang Sun,^{1,6} Yingzhao Huang,^{2,3,4,6} Sen Zhao,^{2,3,4} Junhui Zhao,¹ Zihui Yan,^{2,3,4} Yang Guo,¹ Mao Lin,^{2,3,4} Wenyao Zhong,¹ Yuehan Yin,¹ Zefu Chen,^{2,3,4} Nan Zhang,¹ Yuanqiang Zhang,^{2,3,4} Zongxuan Zhao,¹ Qingyang Li,¹ Lianlei Wang,^{2,3,4} Xiying Dong,^{2,3,4} Yaqi Li,^{2,3,4} Xiaoxin Li,^{3,5} Guixing Qiu,^{2,3,4} DISCO (Deciphering Disorders Involving Scoliosis & COmorbidities) study group, Terry Jianguo Zhang,^{2,3,4} Zhihong Wu,^{3,4,5} Wen Tian,¹ and Nan Wu^{2,3,4}

¹Department of Hand Surgery, Beijing Jishuitan Hospital, Beijing 100035, China; ²Department of Orthopedic Surgery, State Key Laboratory of Complex Severe and Rare Diseases, Peking Union Medical College Hospital, Peking Union Medical College and Chinese Academy of Medical Sciences, Beijing 100730, China; ³Beijing Key Laboratory for Genetic Research of Skeletal Deformity, Beijing 100730, China; ⁴Key Laboratory of Big Data for Spinal Deformities, Chinese Academy of Medical Sciences, Beijing 100730, China; ⁵Medical Research Center, State Key Laboratory of Complex Severe and Rare Diseases, Peking Union Medical College Hospital, Peking Union Medical College and Chinese Academy of Medical Sciences, Beijing 100730, China

Congenital limb malformations (CLMs) affect 1 in 500 live births. However, the value of exome sequencing (ES) for CLM is lacking. The purpose of this study was to decipher the mutational signature of CLM on an exome level. We enrolled a cohort of 66 unrelated probands (including 47 families) with CLM requiring surgical correction. ES was performed for all patients and available parental samples. A definite molecular diagnosis was achieved in 21 out of 66 (32%) patients. We identified 19 pathogenic or likely pathogenic single-nucleotide variants and three copy number variants, of which 11 variants were novel. We identified four variants of uncertain significance. Additionally, we identified *RPL9* and *UBA2* as novel candidate genes for CLM. By comparing the detailed phenotypic features, we expand the phenotypic spectrum of diastrophic dysplasia and chromosome 6q terminal deletion syndrome. We also found that the diagnostic rate was significantly higher in patients with a family history of CLM ($p = 0.012$) or more than one limb affected ($p = 0.034$). Our study expands our understanding of the mutational and phenotypic spectrum of CLM and provides novel insights into the genetic basis of these syndromes.

INTRODUCTION

Congenital limb malformation (CLM) represents a heterogeneous group of structural abnormalities of the limbs that originate from perturbations during limb development. CLM affects ~1 in 500 live births.^{1,2} While CLM is usually isolated, it can be present in conjunction with other congenital syndromes, such as Apert syndrome,³ Duane-radial ray syndrome,⁴ and Holt-Oram syndrome.⁵ About 20% of individuals with CLMs have at least one associated anomaly, and 10% of all congenital anomalies have upper limb involvement.⁶ Along with coexisting anomalies, CLM presents a significant psychological and clinical burden to affected individuals and their families.

Several types of genetic variants, including single-nucleotide variants (SNVs), small insertions and deletions (indels), and copy number variants (CNVs), have been implicated in CLM. The establishment of a genetic profile is essential to providing accurate genetic diagnosis and counseling, and to allow better understanding of disease prognosis. Despite the fact that there are >500 genes associated with CLM, many candidate genes remain under-recognized, and the majority of CLM cases cannot be diagnosed on a molecular level.⁷

In order to investigate the molecular basis of CLM on an exome level, we performed exome sequencing (ES) in a cohort of 66 patients with CLM. In addition, to identify the mutational spectrum in known CLM-associated genes, we also searched for potentially novel CLM candidate genes and phenotypic expansions.

RESULTS

Clinical characteristics and diagnostic yield

We enrolled a total of 66 unrelated probands with CLM of Chinese Han ethnicity, including 41 males and 25 females. Forty-seven of them underwent family-based ES. Nineteen cases underwent

Received 14 December 2020; accepted 13 April 2021;
<https://doi.org/10.1016/j.omtn.2021.04.012>.

⁶These authors contributed equally

Correspondence: Nan Wu, Department of Orthopedic Surgery, State Key Laboratory of Complex Severe and Rare Diseases, Peking Union Medical College Hospital, Peking Union Medical College and Chinese Academy of Medical Sciences, Beijing 100730, China.
E-mail: dr.wunan@pumch.cn

Correspondence: Wen Tian, Department of Hand Surgery, Beijing Jishuitan Hospital, Beijing 100035, China.
E-mail: wentianjst@163.com

Correspondence: Zhihong Wu, Medical Research Center, State Key Laboratory of Complex Severe and Rare Diseases, Peking Union Medical College Hospital, Peking Union Medical College and Chinese Academy of Medical Sciences, Beijing 100730, China.
E-mail: orthoscience@126.com



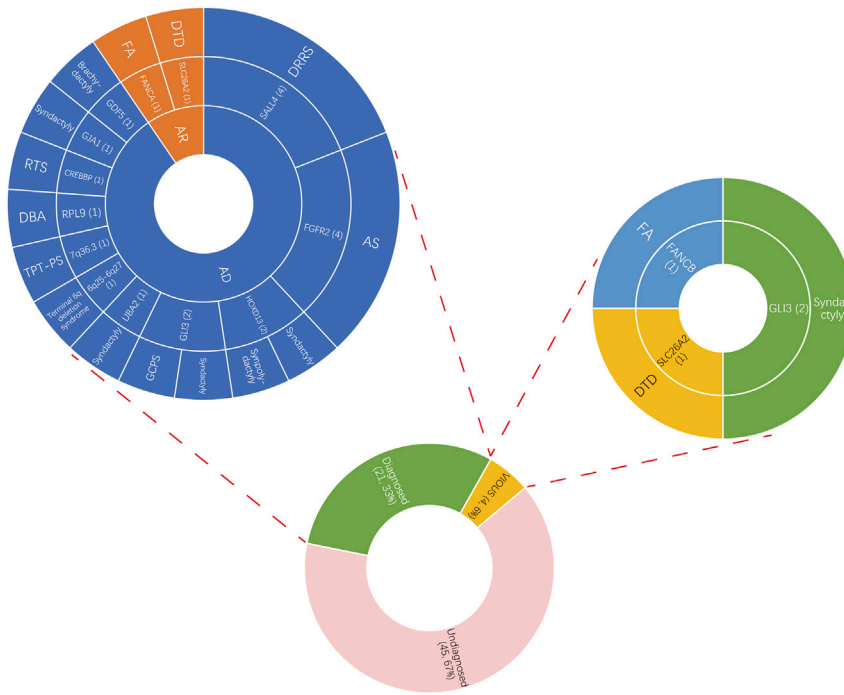


Figure 1. Sunburst chart showing diagnostic yield of the cohort

AD, autosomal dominant; AR, autosomal recessive; AS, Apert syndrome; GCPS, Greig cephalopolysyndactyly syndrome; DBA, Diamond-Blackfan anemia; RTS, Rubinstein-Taybi syndrome; FA, Fanconi anemia; DTD, diagnosis of diastrophic dysplasia; DRRS, Duane-radial ray syndrome; VOUS, variant of uncertain significance.

Pathogenic variants in known disease-causing genes

In total, previously reported causal variants in three genes were observed in six patients: *FGFR2* (n = 4), *GJA1* (n = 1), and *HOXD13* (n = 1) (Table 3), accounting for 9% of all cases in the study (Figure 2). (1) Among these, we identified a heterozygous *FGFR2* variant, c.758C > G (p.Pro253Arg), in patients DISCO-JST13, DISCO-JST39, and DISCO-JST51. Notably, all three patients presented with features characteristic of Apert syndrome, such as craniosynostosis, midface hypoplasia, and syndactyly of the hands and feet. (2) We also found a *de novo* heterozygous *FGFR2* variant, c.755C > G(Ser252Trp), in patient DISCO-JST48, who presented typical features of Apert syndrome. These two *FGFR2* variants have been reported in multiple patients with Apert syndrome.^{3,8} Interestingly, an in-frame insertion variant of *RYR1*, c.12788_12793dup (Glu4263_Gly4264dup), was also observed in patient DISCO-JST48, as well as in his father and sister. Patient DISCO-JST48 had a history of malignant hyperthermia during surgery 2 years prior to this study. This c.12788_12793dup (Glu4263_Gly4264dup) has not been previously reported in the literature but occurred four times as a heterozygous mutation in the Genome Aggregation Database (gnomAD) database. However, patient DISCO-JST48's father and sister had no history of anesthesia and no signs of malignant hyperthermia. Thus, this variant is considered a VOUS. (3) A heterozygous *GJA1* c.119C > T (p.Ala40Val) variant was found in patient DISCO-JST22, who presented with syndactyly and dental dysplasia. This variant has previously been found in one Japanese patient with oculodentodigital dysplasia.⁹ (4) Patient DISCO-JST33, who presented with central synpolydactyly, was found to carry a *HOXD13* c.917G > A (p.Arg306Gln) variant, which has previously been identified in multiple patients with synpolydactyly.^{10,11}

proband-only ES. The mean age was 4.01 ± 0.58 years, with the majority (95%) being younger than 10 years old. Reduction anomalies were the most common anomaly in the cohort (25/66, 38%), followed by syndactyly (16/66, 24%), polydactyly (16/66, 24%), brachydactyly (6/66, 9%), and other unclassified anomalies (3/66, 5%). Overall, the characteristics of the cohort reflect a diverse distribution of surgically corrected CLM cases in clinical practice.

In total, 66 probands with CLM were analyzed. Of these, we established a molecular diagnosis in 21 patients (32%) (Figure 1). We identified three CNVs and 19 SNVs located in 10 genes (*SALL4*, *SLC26A2*, *RPL9*, *FANCA*, *FGFR2*, *GLI3*, *HOXD13*, *UBA2*, *GJA1*, and *GDF5*). All together, we identified 19 disease-causing SNVs (including 6 missense, 6 frameshift, 3 splice site, 1 nonsense, and 3 in-frame insertion) and 3 disease-causing CNVs (including deletion of 6q25.3, duplication of 7q36.3, and deletion of 16q24.3). Four variants of unknown significance (VOUS) were found in *GLI3*, *FANCB*, and *SLC26A2*. Among them, diagnostic yield was highly variable among different phenotypic groups (Table 1).

In our cohort, 32 cases (48%) have one limb affected and 34 cases (52%) have more than one limb affected. Thirty-four cases (52%) have syndromic anomalies, and 32 cases (48%) have isolated CLM. Fifty-one cases (77%) are sporadic, and 15 cases (23%) have a positive family history (Table 2). Diagnostic yield was higher in familial cases (60% versus 24%, $p = 0.012$) and cases with more than one limb affected (43% versus 16%, $p = 0.034$) (Table 2). Pathogenic and likely pathogenic variants and VOUS identified in the cohort are summarized in Table 3.

Novel variants in known disease-causing genes

In order to expand our understanding of the mutational landscape of CLM, we focused on novel variants that have not been previously implicated in CLM. We identified nine novel truncating variants in five genes: *SALL4* (n = 4), *GLI3* (n = 2), *SLC26A4* (n = 1), *FANCA* (n = 1), and *CREBBP* (n = 1) (Figure 2). These variants include six frameshift variants, two splice variants, and one nonsense variant. Pedigree, clinical pictures, and results of Sanger sequencing of these

Table 1. Diagnostic yield among different phenotypic groups

	Total (no.)	Diagnosed (no.)	Undiagnosed (no.)	Diagnostic yield (%)	Genes (no. of patients)
Reduction anomaly	25	7	18	28	
Duane-radial ray syndrome	7	4	3	57	<i>SALL4</i> (4)
SHFM	3	0	3	0	
Holt-Oram syndrome	2	0	0	0	
Longitudinal reduction	2	0	2	0	
Epiphyseal dysplasia	1	1	0	100	<i>SLC26A2</i> (1)
Diamond-Blackfan anemia	1	1	0	100	<i>RPL9</i> (1)
Fanconi anemia	1	1	0	100	<i>FANCA</i> (1)
Nager syndrome	1	0	1	0	
Unclassified radial reduction	7	0	7	0	
Syndactyly	16	8	8	50	
Apert syndrome	4	4	0	100	<i>FGFR2</i> (4)
Unclassified	12	4	8	33	<i>GLI3</i> (1); <i>HOXD13</i> (1); <i>GJA1</i> (1); <i>UBA2</i> (1)
Polydactyly	16	6	10	38	
Preaxial polydactyly	10	2	8	20	6q25.3-6q27 deletion (1); 7q36.3 duplication(1)
Postaxial polydactyly	2	0	0	0	
Synpolydactyly	2	2	0	100	<i>HOXD13</i> (2)
Greig cephalopolysyndactyly syndrome	1	1	0	100	<i>GLI3</i> (1)
Rubinstein-Taybi syndrome	1	1	0	100	<i>CREBBP</i> (1)
Brachydactyly	6	1	5	17	
Poland anomaly	5	0	5	0	
Brachydactyly type C	1	1	0	100	<i>GDF5</i> (1)
Others	3	0	2	33	
Constraint band syndrome	2	0	2	0	
Madelung deformity	1	0	1	0	
Total	66	21	45	32	

SHFM, split hand/foot malformation; No., number.

families are presented in [Figure 3](#). Notably, one novel missense variant and one novel in-frame insertion variant were observed in two patients ([Table 3](#)).

A heterozygous *GDF5* c.932T > C (p.Leu311Pro) variant was identified in patient DISCO-JST17 and her mother, both of whom presented with brachydactyly type C (BDC) ([Figure 3C](#)). Two additional family members of patient DISCO-JST17's mother also presented with similar phenotypes, but genetic tests were not performed. This variant is absent from the gnomAD database and is predicted to be deleterious by multiple bioinformatic tools (CADD = 19.42, SIFT = 0, gerp++ = 4.75 and PolyPhen2 HDIV = 0.997). Thus, we considered *GDF5* c.932T > C (p.Leu311Pro) to be a likely pathogenic variant.

Patient DISCO-JST57 had syndactyly of 3rd and 4th fingers of the right hand ([Figure 3H](#)). In addition, her mother and five family members within her mother's family presented with bilateral 2nd toe clinodactyly. ES of the proband and her parents identified an in-frame insertion variant, c.183_203dup (p.Ala65_Ala71dup), in *HOXD13*, which

is absent from the gnomAD database. This variant causes the number of residues in a polyaniline tract of *HOXD13* to increase from 15 to 22. Although this cDNA change was not reported previously, different cDNA changes leading to the polyaniline tract increasing from 15 to 22 residues were observed in several families with syndactyly or clinodactyly.¹²

Phenotypic spectrum expansion in known CLM genes

In our cohort, phenotypic expansion was associated with one gene (*SLC26A2*) and one CNV (6q25.3-6q27). Patient DISCO-JST8 presented with limb shortening, intrauterine growth retardation, language retardation, decreased testicular size, and normal skull size. ES found that DISCO-JST8 carried two *SLC26A2* variants ([Figure 3B](#)). The c.1512G > A (p.Met504Ile) was inherited from his father, and the c.136_137insTT (p.Asp46Valfs*44) was not inherited from his father (mother not tested). Genotype and phenotype of patient DISCO-JST8 strongly suggest the diagnosis of diastrophic dysplasia (DTD), although we are unable to determine whether the variants occur in *trans* or in *cis* because of the unavailability

Table 2. Diagnostic yield comparison in patients with different clinical characteristics

	Total (no.)	Diagnosed (no.)	Undiagnosed (no.)	Diagnostic yield (%)
Family history				
Yes	15	9	6	60
No	51	12	39	24
p value	0.012			
No. of affected limb(s)				
1	32	5	27	16
≥ 2	34	16	21	43
p value	0.034			
Systemic anomalies				
Syndromic	34	13	21	38
Isolated	32	8	24	25
p value	0.297			
No., number.				

of the mother's sample. Typical features of DTD include limb shortening, normal-sized skull, hitchhiker thumbs, and spinal deformities,¹³ whereas language retardation and testicle hypoplasia are not associated with DTD.

Patient DISCO-JST9 presented with congenital heart disease, developmental delay, structural brain anomalies, craniofacial anomalies, constipation, preaxial polydactyly, and elevated blood ketone bodies and dicarboxylic acid level (Figure 3L). CNV analysis through ES identified a heterozygous deletion of 6q25.3-6q27 in patient DISCO-JST9. Although terminal deletion of chromosome 6q (6q25.3-6q27 in this case) is associated with variable phenotype spectrum, the patient's other symptoms of constipation, preaxial polydactyly, and elevated blood ketone bodies and dicarboxylic acid levels have not been previously reported as manifestations of chromosome 6q deletion.¹⁴

Identification of novel candidate genes for CLM

In order to uncover novel genes potentially contributing to CLM, we searched for new candidate genes that have not been reported in CLM. As a result, we identified a *de novo* heterozygous start-loss variant, c.-2+2T > A, in *RPL9* from patient DISCO-JST24, a 2-year-old female born to healthy parents (Figure 3J). This variant was absent from the gnomAD database. The patient presented with bilateral thumb hypoplasia, cleft palate, dental dysplasia, micrognathia, high scapula, and mild anemia (Figure 3J). She is clinically diagnosed with Diamond-Blackfan anemia (DBA), which is an inherited bone marrow failure disorder, along with a number of other systemic anomalies, including thumb hypoplasia and craniofacial defects. Although other members of the ribosomal protein family, such as RPS10 and RPS26, have been associated with DBA,¹⁵ *RPL9*, which encodes ribosomal protein L9, is not an established disease gene. Considering the biological association between *RPL9* and other ribo-

somal proteins, the truncating variant observed in patient DISCO-JST24 provides evidence supporting a causal role of *RPL9* in DBA.

Patient DISCO-JST19 was a 3-year-old male born with an aplasia cutis lesion at vertex, which is ~5 cm in diameter (Figure 3K). His weight and height at 3 years old were 12 kg (<3 SD) and 86 cm (<3 SD), respectively. He had cutaneous syndactyly of 3rd and 4th fingers in the right hand (Figure 3K), which was corrected by a syndactyly release surgery. After the surgery, he developed contractures in these two fingers. Other anomalies include hypospadias and large and low-set ears. He had no Duane anomaly and strabismus. His developmental milestone was normal. Review of his family members revealed no history of aplasia cutis congenita (ACC), digital anomalies, or other syndromes. ES identified a *de novo* heterozygous variant, c.811A > T(p.Lys271Ter), in the *UBA2* gene (Figure 3K). This is predicted to lead to a premature stop codon and is absent from the gnomAD database.

DISCUSSION

By applying ES in a cohort of 66 CLM patients, we found that 21/66 (32%) families within our cohort could be molecularly diagnosed. We identified six known and 11 novel pathogenic/likely pathogenic variants in known CLM-associated genes and revealed two potential novel candidate genes. Additionally, we observed phenotypic expansions for one known CLM-associated gene and CNV.

Limb development is a multi-stage process, which is orchestrated by complex interactions between different signaling pathways. Studies have found that multiple biological pathways are critically involved in the development of limbs.^{16,17} Any perturbation of these pathways could result in CLM. For example, mutations in the WNT pathways have been shown to lead to Robinow syndrome, which is characterized by brachydactyly.^{18,19} Mutations in Cohesin proteins could result in Cornelia de Lange syndrome, which presents clinodactyly and oligodactyly, in the context of limb anomaly.²⁰ Besides genes with sufficient knowledge to be classified in certain biological pathways, many CLM-related genes are still not well studied.

With the advent of high-throughput sequencing technology, >500 CLM-related genes have been identified.²¹ The genetic bases of different kinds of CLM differ from each other but also share some similarities. The majority of polydactyly is caused by mutations in *GLI3*, which could also lead to syndactyly.²² The *HOXD13* mutations can either present clinodactyly or syndactyly, even in the same pedigree.^{10,12} In this study, we identified 19 causal SNVs and three causal CNVs in 66 CLM patients, which reflect the diversity of CLM causative genes. Thus, we suggest using ES as first-line strategy to identify the genetic basis of CLM.

A previous study used a targeted next-generation sequencing (NGS) strategy encompassing 52 CLM-associated genes along with their regulatory regions in a cohort of 352 CLM patients. They found that 35.2% patients could be molecularly diagnosed,⁷ a rate similar to that in our study. However, we identified a different mutational architecture: only 6 among 15 genes identified in our study were included

Table 3. Summary of pathogenic and likely pathogenic variants identified in the cohort

Known Genes										
CaseID	Limb presentations	Systemic features	Family history	No. of affected limbs	Locus	Zygoty	cDNA change	Protein change	ACMG grade	Reference (PMID)
DISCO-JST1	reduction anomaly	Y	Y	B-H	<i>SALL4</i>	Het	c.1823del	p.Asn608Thrfs*2	P	this study
DISCO-JST8	reduction anomaly	Y	N	B-H, B-F	<i>SLC26A2</i>	NA ^a	c.136_137insTT	p.Asp46Valfs*44	P	this study
DISCO-JST13	syndactyly	Y	N	B-H, B-F	<i>FGFR2</i>	Het	c.758C > G	p.Pro253Arg	P	7719344
DISCO-JST17	brachydactyly	N	Y	B-H	<i>GDF5</i>	Het	c.932T > C	p.Leu311Pro	LP	this study
DISCO-JST22	syndactyly	Y	Y	B-H, L-F	<i>GJA1</i>	Het	c.119C > T	p.Ala40Val	P	25327171 and 15879313
DISCO-JST28	polydactyly	Y	N	B-H, B-F	<i>GLI3</i>	Het	c.1474del	p.Asp492Thrfs*10	P	this study
DISCO-JST29	reduction anomaly	Y	N	B-H	<i>FANCA</i>	Hemi	c.3537+2T > C	p.?	P	this study
DISCO-JST33	synpolydactyly	N	Y	R-H	<i>HOXD13</i>	Het	c.917G > A	p.Arg306Gln	P	22374128 and 24789103
DISCO-JST39	syndactyly	Y	N	B-H, B-F	<i>FGFR2</i>	Het	c.758C > G	p.Pro253Arg	P	7719344
DISCO-JST41	reduction anomaly	Y	Y	B-H	<i>SALL4</i>	Het	c.595del	p.Asp199Metfs*41	P	this study
DISCO-JST47	reduction anomaly	Y	Y	B-H	<i>SALL4</i>	Het	c.2462-1G > T	p.?	P	this study
DISCO-JST48	syndactyly	Y	N	B-H, B-F	<i>FGFR2; RYR1</i>	Het; Het	c.755C > G;c.12788_12793dup	p.Ser252Trp; p.Glu4263_Gly4264dup	P; VOUS	7719344; this study
DISCO-JST51	syndactyly	Y	N	B-H, B-F	<i>FGFR2</i>	Het	c.758C > G	p.Pro253Arg	P	7719344
DISCO-JST57	syndactyly	N	Y	R-H	<i>HOXD13</i>	Het	c.183_203dup	p.Ala65_Ala71dup	P	this study
DISCO-JST70	syndactyly	N	N	B-H, B-F	<i>GLI3</i>	Het	c.480del	p.Ala161Profs*55	P	this study
DISCO-JST72	reduction anomaly	Y	Y	R-H	<i>SALL4</i>	Het	c.1746_1747delinsTGTGGG	p.Lys582Asnfs*17	P	this study
DISCO-JST74	broad thumbs	Y	N	R-H	<i>CREBBP</i>	Het	c.4471C > T	p.Gln1491*	P	this study
Novel candidate genes										
CaseID	Limb presentations	Systemic features	Family history	Affected site	Locus	Zygoty	cDNA change	Protein change	gnomAD MAF	
DISCO-JST24	reduction anomaly	Y	N	B-H	<i>RPL9</i>	Het	c.-2+2T > A	p.?	0	
DISCO-JST19	syndactyly	N	N	R-H	<i>UBA2</i>	Het	c.811A > T	p.Lys271Ter	0	

(Continued on next page)

Table 3. Continued

Structural variants										
Case ID	Limb presentations	Systemic features	Family history	Affected site	Locus	Zygoty	Dosage	cDNA change	Protein change	gnomAD MAF
DISCO-JST9	polydactyly	Y	N	R-H	6q25-q27	Het	deletion			
DISCO-JST23	polydactyly	N	Y	B-H	7q36.3	Het	duplication			
DISCO-JST29	reduction anomaly	Y	N	B-H	16q24.3	Het	deletion			
VOUS										
CaseID	Limb presentations	Systemic features	Family history	Affected site	Locus	Zygoty	cDNA change	Protein change	gnomAD MAF	
DISCO-JST35	syndactyly	N	N	L-H	GLI3	Het	c.103G > A	p.Ala35Thr	0	
DISCO-JST38	polydactyly	Y	N	R-H	FANCB	Het	c.2166-8delT	p?	0	
DISCO-JST55	syndactyly	N	N	R-H	GLI3	Het	c.3415G > T	p.Ala139Ser	4.01E-06	
DISCO-JST8	reduction anomaly	Y	N	B-H, B-F	SLC26A2	NA*	c.1512G > A	p.Met504Ile	2.76E-4	

Y, yes or present; N, not present; No, number; H, hand; F, foot; Het, heterozygous; B, bilateral; R, right; L, left; Hom, homozygous; P, pathogenic; LP, likely pathogenic; VOUS, variant of unknown significance; MAF, minor allele frequency; NA, not available.

*Due to lack of maternal sample, the zygosity cannot be determined.

in the reported panel. Indeed, there is epidemiological variation of CLM among different regions and demographics,^{2,21,23} which might explain the difference of mutational architecture. Using a targeted NGS strategy is time-saving in clinical practice. However, >500 genes are associated with CLM, and the genetic cause of CLM remains largely elusive. Using an exome-wide or genome-wide strategy has the potential to establish an unbiased genetic landscape and uncover novel candidate genes.

In our cohort, we found that the diagnostic yield was higher in familial cases and cases with more than one limb affected (Table 2). Previous studies have drawn similar conclusions regarding the existence of family history and systemic abnormalities and the ability of these factors to affect diagnostic yield.⁷ In this study, we describe for the first time how the number of affected limbs can influence the diagnostic yield. This might be helpful for clinical geneticists to provide precise management of patients with CLM.

We identified a start-lost variant in *RPL9*, which is not a well-established disease gene. Previously, this *RPL9* variant has only been found in one patient with DBA.¹⁵ Since the phenotypic manifestation of our patient is highly similar to DBA, and DBA is caused by variants in the ribosomal protein family with only a few exceptions, we concluded that *RPL9* may represent a potential novel disease gene candidate for DBA.²⁴ Additionally, the variant leads to start-loss of *RPL9* protein, and the probability of loss-of-function intolerance (pLI) score of *RPL9* is 0.96. Nevertheless, further studies are still needed to confirm the relationship between *RPL9* and DBA.

We identified a *de novo* nonsense *UBA2* variant in a patient with ACC, intrauterine and postnatal growth retardation, syndactyly, atrial septal defect, hypospadias, and large and low-set ears. These phenotypes are also typical features in 19q13.11 deletion syndrome.²⁵ Among patients with 19q13.11 deletion, most of them had ACC and most male patients had underdelivered genitalia, as observed in our case. After analyzing the correlation between clinical features and deleted regions, Melo et al.²⁶ hypothesized that haploinsufficiency of *UBA2* gene is responsible for ACC. This hypothesis was further supported by the identification of *UBA2* variants in ACC patients. Marble et al.²⁷ reported a patient with ACC, Duane anomaly, and hip dysplasia, who carried a *de novo* missense variant c.71G > T (p.Gly24Val) in *UBA2*. Wang et al.²⁸ reported a male child and his mother both affected with ACC and found to have a co-segregating truncating variant, c.327delT(p.Phe109Leufr*5), while, in a recent study about split-hand/foot malformation, Yamoto et al.²⁵ identified a *UBA2* frameshift variant, c.1324dupT p.(Tyr442Leufs*17), in a patient affected with split hand/foot malformation but not ACC. Our findings strengthen the hypothesis that *UBA2* is a novel candidate gene for Mendelian ACC and provide novel insights in relating *UBA2* with syndactyly.

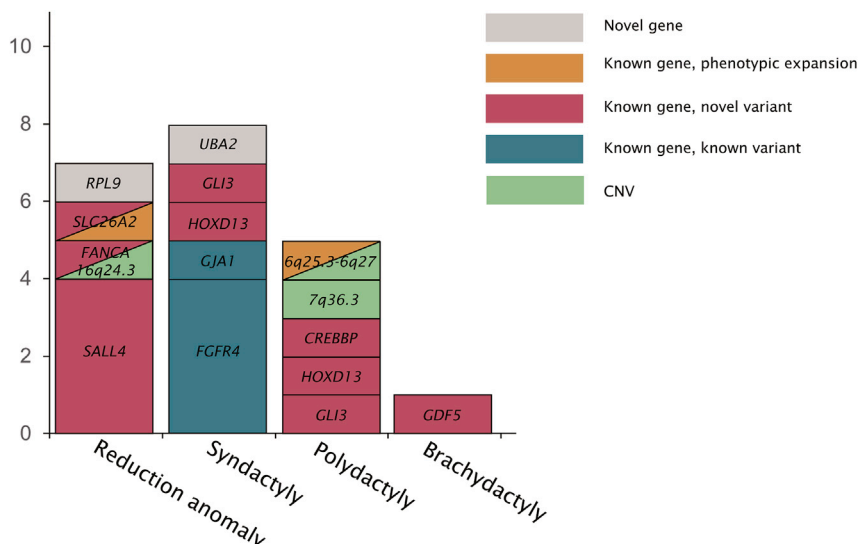


Figure 2. Distribution of the disease genes in 66 families with established molecular diagnosis by phenotypic groups

Exome sequencing and data processing

In brief, DNA samples were prepared into Illumina paired-end libraries and underwent whole-exome capture with the Agilent V5, followed by sequencing on the Illumina HiSeq 4000 platform (Illumina, San Diego, CA, USA). In-house-developed Peking Union Medical College Hospital Pipeline (PUMP) was used for variant calling and annotation.^{29,30}

An in-house control dataset of 100 exomes was incorporated for CNV analysis. Coverage information was computed from BAM files with GATK. Then, unqualified targets with fewer than 50% samples covered or with a mean coverage under 10× were filtered out. After quality control, read depths for each sample were analyzed and a Z score was calculated. CNVs were called according to the Z score.

ES data interpretation

Rare variants with minor allele frequencies < 0.01 in 1000 Genomes (October 2013), gnomAD (<https://gnomad.broadinstitute.org>), the Exome Aggregation Consortium (ExAC; <http://exac.broadinstitute.org>), and the in-house database of Deciphering Disorders Involving Scoliosis and COmorbidities (DISCO, <http://discostudy.org/>, >2,000 exomes) were extracted. First, we examined disease-causing variants in previously reported candidate genes and CNVs. Variant classification was conducted according to American College of Medical Genetics and Genomics (ACMG) guidelines.³¹

For patients highly suspected of a specific syndrome but without a previously identified pathogenic/likely pathogenic variant, we prioritized potential new variant(s) in the disease-associated gene(s). First, truncating variants in genes predicted to be intolerant to loss-of-function changes according to the gnomAD (pLI score ≥ 0.9) were identified as susceptibility variants. Variants that are predicted with a CADD score of >15 were presumed damaging. Candidacy of rare and damaging variants was further evaluated by their known gene function, animal models, and association with known CLM genes.

Validation of candidate variants

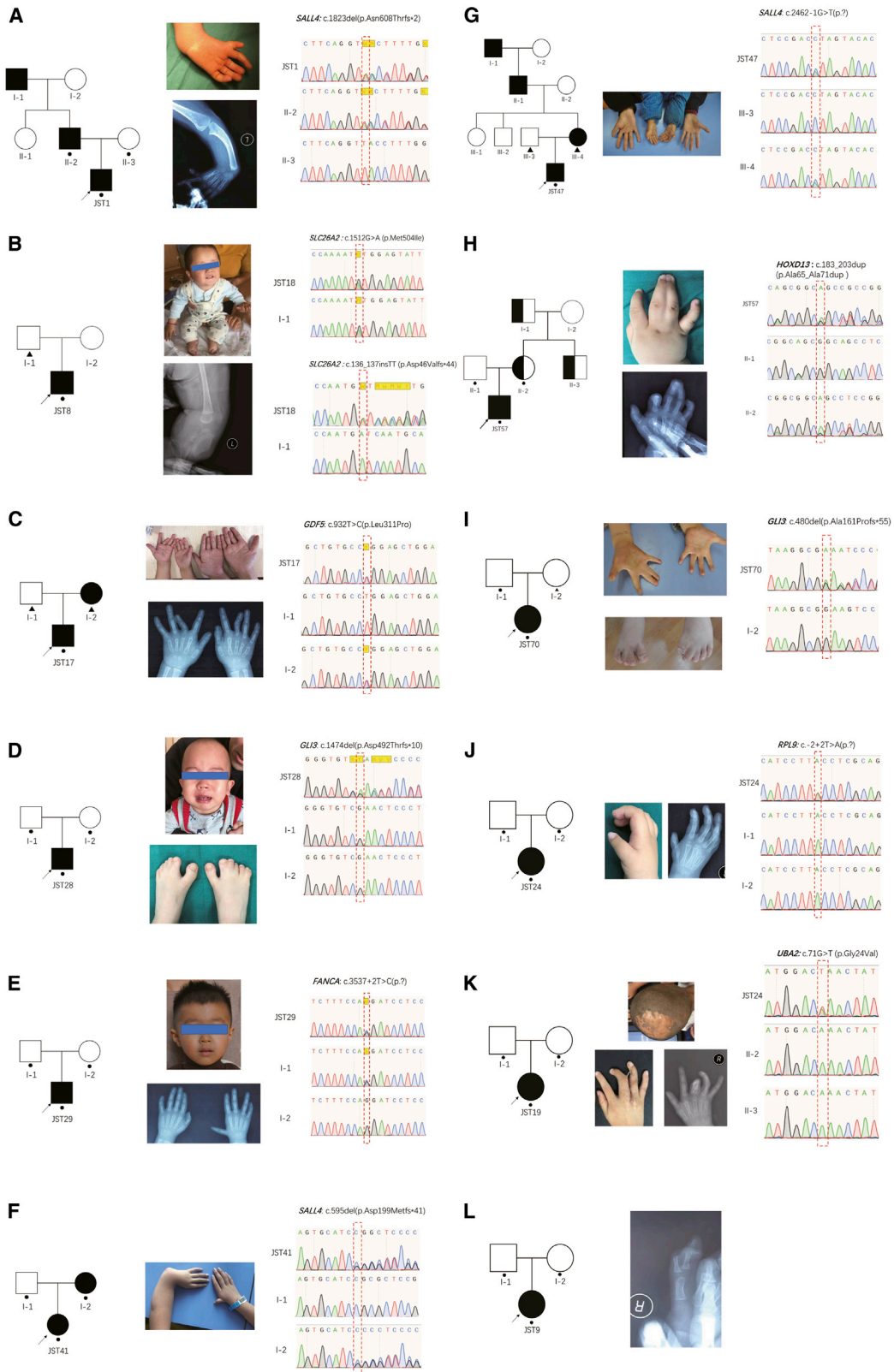
Variant-encoding amplicons were amplified by PCR from genomic DNA obtained from subjects, purified with an Axygen AP-GX-50 kit (lot no. 05915KE1), and sequenced by Sanger sequencing on an ABI3730XL instrument.

All together, we performed ES on a cohort of 66 Chinese patients with CLM. Our findings of previously reported variants confirmed the pathogenicity of those variants and the validity of our protocol. We also found several novel variants that expand the mutational architecture. Finally, we identified *RPL9* and *UBA2* as possible novel candidate genes for CLM.

MATERIALS AND METHODS

Cohort recruitment and sample preparation

In this study, we enrolled a total of 66 unrelated probands with surgical corrective CLM admitted to Beijing Jishuitan Hospital, China from April 2018 to September 2019 as a part of the Deciphering disorders Involving Scoliosis and COmorbidities study (<http://www.discostudy.org/>), as well as 47 pairs of patient parents. Medical records, X-rays, clinical images, and blood samples were collected for each patient. Limb and systemic anomalies of these patients were evaluated by experienced hand surgeons and pediatricians. Patients were classified into five phenotypic groups. The reduction anomaly group included patients with Duane-radial ray syndrome, split hand/foot malformation, Holt-Oram syndrome, multiple epiphyseal dysplasia, DBA, Fanconi anemia, and unclassified radial anomalies. The syndactyly group consisted of patients with Apert syndrome and isolated syndactyly (unclassified). The polydactyly group included patients with preaxial polydactyly, postaxial polydactyly, synpolydactyly, Greig cephalopolysyndactyly syndrome (GCPS), and Rubinstein-Taybi syndrome (RTS). The brachydactyly group included patients with Poland anomaly and BDC. Several other conditions were also screened in our cohort, including constraint band syndrome and Madelung deformity. After collection of blood samples, genomic DNA was extracted with the DNeasy Blood & Tissue Kit (QIAGEN, Germany) according to the manufacturer's protocol. This study was approved by the ethics committee of Beijing Jishuitan Hospital. Informed consent was obtained from each patient or their parents.



(legend on next page)

Statistics

SPSS Statistics v.15.0 software was used for statistical analyses, and a p value < 0.05 was considered statistically significant.

ACKNOWLEDGMENTS

We thank the families who participated in this research. This research was funded in part by the National Key Research and Development Program of China (2016YFC0901500); Center for Rare Diseases Research, Chinese Academy of Medical Sciences, Beijing, China (2016ZX310174-4); Beijing JST Research Funding (ZR-201907 and 2019-YJ03); Beijing Jishuitan Hospital Nova Program (XKXX201818); National Natural Science Foundation of China (81822030, 82072391, 81672123, 81972037, 81772299, 81930068, 81772301, and 81972132); Non-profit Central Research Institute Fund of Chinese Academy of Medical Sciences (no. 2019PT320025); Beijing Natural Science Foundation (JQ20032 and 7191007); Tsinghua University-Peking Union Medical College Hospital Initiative Scientific Research Program; CAMS Initiative Fund for Medical Sciences (2016-I2M-3-003, 2016-I2M-2-006, and 2017-I2M-2-001); and the National Students Innovation and Entrepreneurship Training Program (2019zlgc0609). This work was performed in Beijing, China.

AUTHOR CONTRIBUTIONS

Conceptualization: W.T., Z.W., T.J.Z., and N.W.; cohort enrollment: L.S., Y.G., M.L., Z.Z., Q.L., Y.Y., N.Z., W.Z., and Y.H.; funding acquisition: N.W., Z.W., W.T., and T.J.Z.; experiments: Z.C., L.W., Y.Z., Y.L., and Y.H.; genetic data analysis: Y.H., L.S., S.Z., Z.Y., and N.W.; bioinformatic analysis: Z.Y., S.Z., and Z.C.; writing – review & editing: T.J.Z., G.Q., J.Z., and Z.W.; data interpretation: Z.W., T.J.Z., and N.W.; writing – original draft: Y.H., L.S., S.Z., J.Z., Z.Y., Y.G., X.D., W.T., and N.W.

DECLARATION OF INTERESTS

The authors declare no competing interests.

REFERENCES

- Giele, H., Giele, C., Bower, C., and Allison, M. (2001). The incidence and epidemiology of congenital upper limb anomalies: a total population study. *J. Hand Surg. Am.* 26, 628–634.
- Ekblom, A.G., Laurell, T., and Arner, M. (2014). Epidemiology of congenital upper limb anomalies in Stockholm, Sweden, 1997 to 2007: application of the Oberg, Manske, and Tonkin classification. *J. Hand Surg. Am.* 39, 237–248.
- Wilkie, A.O.M., Slaney, S.F., Oldridge, M., Poole, M.D., Ashworth, G.J., Hockley, A.D., Hayward, R.D., David, D.J., Pulleyn, L.J., Rutland, P., et al. (1995). Apert syndrome results from localized mutations of *FGFR2* and is allelic with Crouzon syndrome. *Nat. Genet.* 9, 165–172.
- Al-Baradie, R., Yamada, K., St Hilaire, C., Chan, W.-M., Andrews, C., McIntosh, N., Nakano, M., Martonyi, E.J., Raymond, W.R., Okumura, S., et al. (2002). Duane radial ray syndrome (Okhiro syndrome) maps to 20q13 and results from mutations in *SALL4*, a new member of the SAL family. *Am. J. Hum. Genet.* 71, 1195–1199.
- Basson, C.T., Bachinsky, D.R., Lin, R.C., Levi, T., Elkins, J.A., Soultz, J., Grayzel, D., Kroumpouzou, E., Traill, T.A., Leblanc-Stracessi, J., et al. (1997). Mutations in human *TBX5* [corrected] cause limb and cardiac malformation in Holt-Oram syndrome. *Nat. Genet.* 15, 30–35.
- Arabai, H.M., Farr, A., Bettelheim, D., Weber, M., and Farr, S. (2017). Prenatal diagnosis of congenital upper limb differences: a current concept review. *J. Matern. Fetal Neonatal Med.* 30, 2557–2563.
- Jourdain, A., Petit, F., Odou, M., Balduyck, M., Brunelle, P., Dufour, W., Boussion, S., Brischoux-Boucher, E., Colson, C., Dieux, A., et al. (2020). Multiplex targeted high-throughput sequencing in a series of 352 patients with congenital limb malformations. *Human Mutat* 41, 222–239, 31502745.
- Foldynova-Trantirkova, S., Wilcox, W.R., and Krejci, P. (2012). Sixteen years and counting: the current understanding of fibroblast growth factor receptor 3 (*FGFR3*) signaling in skeletal dysplasias. *Hum. Mutat.* 33, 29–41.
- Hayashi, R., Bito, T., Taniguchi-Ikeda, M., Farooq, M., Ito, M., and Shimomura, Y. (2014). Japanese case of oculodentodigital dysplasia caused by a mutation in the *GJA1* gene. *J. Dermatol.* 41, 1109–1110.
- Debeer, P., Bacchelli, C., Scambler, P.J., De Smet, L., Fryns, J.-P., and Goodman, F.R. (2002). Severe digital abnormalities in a patient heterozygous for both a novel missense mutation in *HOXD13* and a polyalanine tract expansion in *HOXA13*. *J. Med. Genet.* 39, 852–856.
- Dai, L., Liu, D., Song, M., Xu, X., Xiong, G., Yang, K., Zhang, K., Meng, H., Guo, H., and Bai, Y. (2014). Mutations in the homeodomain of *HOXD13* cause syndactyly type I-c in two Chinese families. *PLoS ONE* 9, e96192.
- Kjaer, K.W., Hedeboe, J., Bugge, M., Hansen, C., Friis-Henriksen, K., Vestergaard, M.B., Tommerup, N., and Opitz, J.M. (2002). *HOXD13* polyalanine tract expansion in classical synpolydactyly type Vordingborg. *Am. J. Med. Genet.* 110, 116–121.

Figure 3. Clinical and genetic characteristics of patients carrying novel variants and variants in novel candidate genes

(A) Left, pedigree of DISCO-JST1. Middle, top, right thumb hypoplasia. Middle, bottom, the radiograph reveals left radial hypoplasia. Right, Sanger validation of the *SALL4* variants in DISCO-JST1. (B) Left, pedigree of DISCO-JST8. Middle, top, limb shortening. Middle, bottom, underdeveloped fibula and tibia. Right, Sanger validation of the *SLC26A2* variants in DISCO-JST8. (C) Left, pedigree of DISCO-JST17. Middle, top, brachydactyly of the patient (left side) and his mother (right side). Middle, bottom, brachydactyly and ulna deviation of the middle fingers. Right, Sanger validation of the *GDF5* variants in DISCO-JST17. (D) Left, pedigree of DISCO-JST28. Middle, top, macrocephaly, dental dysplasia, and ear deformities. Middle, bottom, polysyndactyly of both feet. Right, Sanger validation of the *GLI3* variants in DISCO-JST28. (E) Left, pedigree of DISCO-JST29. Middle, top, ear deformities and strabismus. Middle, bottom, radiograph showing thumb hypoplasia. Right, Sanger validation of the *FANCA* variants in DISCO-JST29. (F) Left, pedigree of DISCO-JST41. Middle, severe radial hypoplasia of both sides. Right, Sanger validation of the *SALL4* variants in DISCO-JST41. (G) Left, pedigree of DISCO-JST47. Middle, thumb hypoplasia of the patient (medial) and his mother (lateral). Right, Sanger validation of the *SALL4* variants in DISCO-JST47. (H) Left, pedigree of DISCO-JST57. Middle, top, syndactyly of 3rd and 4th fingers. Middle, bottom, radiograph showing fusion of distal phalanges of 3rd and 4th fingers. Right, Sanger validation of the *HOXD13* variants in DISCO-JST57. (I) Left, pedigree of DISCO-JST70. Middle, top, syndactyly of right 2nd, 3rd, and 4th fingers. Middle, bottom, syndactyly of right 2nd and 3rd toes, left 1st, 2nd, and 3rd toes. Right, Sanger validation of the *GLI3* variants in DISCO-JST70. (J) Left, pedigree of DISCO-JST24. Middle, left, right thumb hypoplasia. Middle, right, radiograph showing right thumb hypoplasia. Right, Sanger validation of the *RPL9* variants in DISCO-JST24. (K) Left, pedigree of DISCO-JST19. Middle, top, an aplasia cutis lesion at the vertex. Middle, bottom, syndactyly of right 3rd and 4th fingers. Right, Sanger validation of the *UBA2* variants in DISCO-JST19. (L) Left, pedigree of DISCO-JST9. Right, X-ray showing right hand polydactyly. “●” indicates this individual underwent exome sequencing and Sanger sequencing. ▲ indicates this individual underwent Sanger sequencing only.

13. Al Kaissi, A., Kenis, V., Melchenko, E., Chehida, F.B., Ganger, R., Klaushofer, K., and Grill, F. (2014). Corrections of lower limb deformities in patients with diastrophic dysplasia. *Orthop. Surg.* 6, 274–279.
14. De Cinque, M., Palumbo, O., Mazzucco, E., Simone, A., Palumbo, P., Ciavatta, R., Maria, G., Ferese, R., Gambardella, S., Angiolillo, A., et al. (2017). Developmental Coordination Disorder in a Patient with Mental Disability and a Mild Phenotype Carrying Terminal 6q26-qter Deletion. *Front. Genet.* 8, 206.
15. Doherty, L., Sheen, M.R., Vlachos, A., Choemmel, V., O'Donohue, M.-F., Clinton, C., Schneider, H.E., Sieff, C.A., Newburger, P.E., Ball, S.E., et al. (2010). Ribosomal protein genes RPS10 and RPS26 are commonly mutated in Diamond-Blackfan anemia. *Am. J. Hum. Genet.* 86, 222–228.
16. Pignatti, E., Zeller, R., and Zuniga, A. (2014). To BMP or not to BMP during vertebrate limb bud development. *Semin. Cell Dev. Biol.* 32, 119–127.
17. Lopez-Rios, J. (2016). The many lives of SHH in limb development and evolution. *Semin. Cell Dev. Biol.* 49, 116–124.
18. Person, A.D., Beiraghi, S., Sieben, C.M., Hermanson, S., Neumann, A.N., Robu, M.E., Schleiffarth, J.R., Billington, C.J., van Bokhoven, H., Hoogeboom, J.M., et al. (2009). *WNT5A* mutations in patients with autosomal dominant Robinow syndrome. *Dev. Dyn.* 239, 327–337, 19918918.
19. Woods, C.G., Stricker, S., Seemann, P., Stern, R., Cox, J., Sherridan, E., Roberts, E., Springell, K., Scott, S., Karbani, G., et al. (2006). Mutations in *WNT7A* cause a range of limb malformations, including Fuhrmann syndrome and Al-Awadi/Raas-Rothschild/Schinzel phocomelia syndrome. *Am. J. Hum. Genet.* 79, 402–408.
20. Deardorff, M.A., Wilde, J.J., Albrecht, M., Dickinson, E., Tennstedt, S., Braunholz, D., Mönnich, M., Yan, Y., Xu, W., Gil-Rodríguez, M.C., et al. (2012). *RAD21* mutations cause a human cohesinopathy. *Am. J. Hum. Genet.* 90, 1014–1027.
21. Mano, H., Fujiwara, S., Takamura, K., Kitoh, H., Takayama, S., Ogata, T., Hashimoto, S., and Haga, N. (2018). Congenital limb deficiency in Japan: a cross-sectional nationwide survey on its epidemiology. *BMC Musculoskelet. Disord.* 19, 262.
22. Al-Qattan, M.M., Shamseldin, H.E., Salih, M.A., and Alkuraya, F.S. (2017). *GLI3*-related polydactyly: a review. *Clin. Genet.* 92, 457–466.
23. Carli, D., Fairplay, T., Ferrari, P., Sartini, S., Lando, M., Garagnani, L., Di Gennaro, G.L., Di Pancrazio, L., Bianconi, G., Elmakky, A., et al. (2013). Genetic basis of congenital upper limb anomalies: analysis of 487 cases of a specialized clinic. *Birth Defects Res. A Clin. Mol. Teratol.* 97, 798–805.
24. Da Costa, L., Narla, A., and Mohandas, N. (2018). An update on the pathogenesis and diagnosis of Diamond-Blackfan anemia. *F1000Res.* 7, F1000 Faculty Rev-1350.
25. Yamoto, K., Saitsu, H., Nishimura, G., Kosaki, R., Takayama, S., Haga, N., Tonoki, H., Okumura, A., Horii, E., Okamoto, N., et al. (2019). Comprehensive clinical and molecular studies in split-hand/foot malformation: identification of two plausible candidate genes (*LRP6* and *UBA2*). *Eur. J. Hum. Genet.* 27, 1845–1857.
26. Melo, J.B., Estevinho, A., Saraiva, J., Ramos, L., and Carreira, I.M. (2015). Cutis Aplasia as a clinical hallmark for the syndrome associated with 19q13.11 deletion: the possible role for *UBA2* gene. *Mol. Cytogenet.* 8, 21.
27. Marble, M., Guillen Sacoto, M.J., Chikarmane, R., Gargiulo, D., and Juusola, J. (2017). Missense variant in *UBA2* associated with aplasia cutis congenita, duane anomaly, hip dysplasia and other anomalies: A possible new disorder involving the SUMOylation pathway. *Am. J. Med. Genet. A.* 173, 758–761.
28. Wang, Y., Dupuis, L., Jobling, R., and Kannu, P. (2020). Aplasia cutis congenita associated with a heterozygous loss-of-function *UBA2* variant. *Br. J. Dermatol.* 182, 792–794.
29. Wang, K., Zhao, S., Liu, B., Zhang, Q., Li, Y., Liu, J., Shen, Y., Ding, X., Lin, J., Wu, Y., et al. (2018). Perturbations of BMP/TGF- β and VEGF/VEGFR signalling pathways in non-syndromic sporadic brain arteriovenous malformations (BAVM). *J. Med. Genet.* 55, 675–684.
30. Zhao, S., Zhang, Y., Chen, W., Li, W., Wang, S., Wang, L., Zhao, Y., Lin, M., Ye, Y., Lin, J., et al.; Deciphering Disorders Involving Scoliosis and Comorbidities (DISCO) study (2021). Diagnostic yield and clinical impact of exome sequencing in early-onset scoliosis (EOS). *J. Med. Genet.* 58, 41–47.
31. Richards, S., Aziz, N., Bale, S., Bick, D., Das, S., Gastier-Foster, J., Grody, W.W., Hegde, M., Lyon, E., Spector, E., et al.; ACMG Laboratory Quality Assurance Committee (2015). Standards and guidelines for the interpretation of sequence variants: a joint consensus recommendation of the American College of Medical Genetics and Genomics and the Association for Molecular Pathology. *Genet. Med.* 17, 405–424.